J. Membrane Biol. 210, 31–42 (2006)
DOI: 10.1007/s00232-005-7028-2

The Journal of
Membrane
Biology

Interactions between Impermeant Blocking Ions in the Cystic Fibrosis Transmembrane Conductance Regulator Chloride Channel Pore: Evidence for Anion-Induced Conformational Changes

Ning Ge, Paul Linsdell
Department of Physiology and Biophysics, Dalhousie University, Halifax, Nova Scotia B3H 1X5, Canada

Received: 22 December 2005/Revised: 3 February 2006

Abstract. It is well known that extracellular Cl^- ions can weaken the inhibitory effects of intracellular open channel blockers in the cystic fibrosis transmembrane conductance regulator (CFTR) Cl^- channel pore. This effect is frequently attributed to repulsive ion-ion interactions inside the pore. However, since Cl^- ions are permeant in CFTR, it is also possible that extracellular Cl^- ions are directly competing with intracellular blocking ions for a common binding site; thus, this does not provide direct evidence for multiple, independent anion binding sites in the pore. To test for the possible through-space nature of ion-ion interactions inside the CFTR pore, we investigated the interaction between impermeant anions applied to either end of the pore. We found that inclusion of low concentrations of impermeant $Pt(NO_2)_4^{2-}$ ions in the extracellular solution weaken the blocking effects of three different intracellular blockers [$Pt(NO_2)_4^{2-}$, glibenclamide and 5-nitro-2-(3-phenylpropylamino)benzoic acid] without affecting their apparent voltage dependence. However, the effects of extracellular $Pt(NO_2)_4^{2-}$ ions are too strong to be accounted for by simple competitive models of ion binding inside the pore. In addition, extracellular $Fe(CN)_6^{3-}$ ions, which do not appear to enter the pore, also weaken the blocking effects of intracellular $Pt(NO_2)_4^{2-}$ ions. In contrast to previous models that invoked interactions between anions bound concurrently inside the pore, we propose that $Pt(NO_2)_4^{2-}$ and $Fe(CN)_6^{3-}$ binding to an extracellularly accessible site outside of the channel permeation pathway alters the structure of an intracellular anion binding site, leading to weakened binding of intracellular blocking ions.

Correspondence to: P. Linsdell; email: paul.linsdell@dal.ca

Key words: Ion channel — Anion permeation — Ion-ion interaction — Open channel block — Multi-ion pore — Blocker knock-off

Introduction

Biophysical evidence has long suggested that ions bind to specific sites within ion channel pores (Hille, 2001), and this thought has now been strikingly confirmed by the identification of multiple, discrete permeant ion binding sites in the crystal structures of both cation-selective (Doyle et al., 1998; Zhou et al., 2001b) and anion-selective channels (Dutzler, Campbell & MacKinnon, 2003). Simultaneous binding of permeant ions to multiple closely spaced sites within the channel pore, leading to mutual electrostatic repulsion, is thought to be the key link between stringent ionic selectivity and rapid ion translocation in cation-selective channel pores (MacKinnon, 2003; Sather & McCleskey, 2003). Similarly, in both cystic fibrosis transmembrane conductance regulator (CFTR) (Linsdell, 2006) and ClC Cl^- (Dutzler et al., 2003; Cohen & Schulten, 2004) channels, it has been suggested that simultaneous occupancy of multiple anion binding sites in the pore by Cl^- ions leads to repulsive interactions that are a critical part of the normal mechanism of rapid Cl^- ion permeation.

Several different lines of evidence suggest that the CFTR pore is capable of holding more than one anion at a time (Linsdell, 2006). Movement of the permeant anions Cl^- and $Au(CN)_2^-$ appears to be coupled inside the pore (Gong & Linsdell, 2003b), suggesting that anions do not move independently through the pore but instead are sensitive to one another's presence. Entry of $Pt(NO_2)_4^{2-}$ ions from the intracellular solution into the pore of a mutant form of CFTR (F337A) accelerates the exit of other

$Pt(NO_2)_4^{2-}$ ions that are already bound inside the pore (Gong & Linsdell, 2003a). However, the most commonly observed manifestation of so-called multi-ion pore behavior in CFTR is the ability of extracellular Cl^- to disrupt the binding of intracellular open channel blockers inside the pore. Thus, increasing the extracellular Cl^- concentration weakens the blocking effects of intracellular anions such as diphenylamine-2-carboxylate (DPC) (McDonough et al., 1994), gluconate (Linsdell & Hanrahan, 1996b; Linsdell, Tabcharani & Hanrahan, 1997), glibenclamide (Sheppard & Robinson, 1997; Gupta & Linsdell, 2002; Zhou, Hu & Hwang, 2002), taurolithocholate-3-sulfate (Linsdell & Hanrahan, 1999), lonidamine (Gong et al., 2002b), isethionate (Zhou et al., 2002), $Au(CN)_2^-$ (Gong & Linsdell, 2003b), $Pt(NO_2)_4^{2-}$ (Gong & Linsdell, 2003a) and unknown cytosolic anion(s) that appear to block CFTR Cl^- currents in intact cells (Zhou, Hu & Hwang, 2001a). These effects of extracellular Cl^- are usually ascribed to Cl^- ions entering the pore from the outside and binding within it, destabilizing the binding of blocking anions bound to other, more intracellular sites, perhaps by an electrostatic mechanism – the now classical "knock-off" mechanism (MacKinnon & Miller, 1988; Neyton & Miller, 1988). However, since Cl^- itself is permeant, an alternative explanation could be that extracellular Cl^- ions pass most of the way through the pore to bind at the binding site for intracellular blockers, thereby weakening the block by direct competition. As a result, these experiments do not establish whether or not Cl^- and other anions bound at separate sites inside the pore experience through-space interactions.

A better test for through-space interactions inside the pore might come from the study of ions that cannot permeate the channel and, presumably therefore, cannot compete for a common site when applied to opposite ends of the channel. This strategy has been used, for example, to show that interactions do take place between impermeant tetraethylammonium (TEA) ions applied to either end of K^+ channel pores (Newland et al., 1992; Thompson & Begenisich, 2000). In the present study, we test for these kinds of through-space interactions in the CFTR pore using the divalent pseudohalide anion $Pt(NO_2)_4^{2-}$, an impermeant blocker of the pore (Gong & Linsdell, 2003b). This anion blocks Cl^- permeation when applied to either end of the pore (but with a considerably higher affinity from the intracellular side), presumably by binding to separate sites located on different sides of some barrier to $Pt(NO_2)_4^{2-}$ permeation within the pore (Gong & Linsdell, 2003b). In this case, we reason it may be possible to identify interactions between anions bound concurrently to different sites by functional means.

Methods

Experiments were carried out on baby hamster kidney cells stably transfected with wild-type human CFTR (Chang et al., 1998). Macroscopic and single-channel patch-clamp recordings were made from inside-out patches excised from these cells, as described in detail previously (Gong et al., 2002a; Gong & Linsdell, 2003b; Ge et al., 2004). Following patch excision and recording of background currents, CFTR channels were activated by exposure to protein kinase A (PKA) catalytic subunit (1-20 nM) plus magnesium-adenosine triphosphate (MgATP, 1 mM) in the cytoplasmic (bath) solution. As in a previous study (Ge et al., 2004), single-channel currents were recorded following weak PKA stimulation (1–10 nM), whereas all macroscopic CFTR currents were recorded following maximal PKA stimulation (~20 nM) and subsequent treatment with inorganic sodium pyrophosphate (PPi, 2 mM) to "lock" channels in the open state. The intracellular (bath) solution contained (mM): 150 NaCl, 10 *N*-tris[hydroxymethyl]methyl-2-aminoethanesulfonate (TES) and 2 $MgCl_2$. Intracellular blockers were added to this solution from stocks made up in the same buffer; glibenclamide and 5-nitro-2-(3-phenylpropylamino)benzoic acid (NPPB) were initially solubilized in dimethyl sulfoxide (Linsdell, 2005). The extracellular (pipette) solution contained (mM): 150 Na gluconate, 10 TES and 2 $MgCl_2$, to which $K_2Pt(NO_2)_4$ (1-8 mM) or $K_3Fe(CN)_6$ (5 mM) was added as necessary. Higher concentrations of $Pt(NO_2)_4^{2-}$ interfered intolerably with adequate seal formation. All solutions were adjusted to pH 7.4 using NaOH. Given voltages have been corrected for liquid junction potentials, either calculated using pCLAMP9 software (Axon Instruments, Union City, CA) or measured where necessary. All chemicals were from Sigma-Aldrich (Oakville, Canada), except for PKA (Promega, Madison, WI) and $K_2Pt(NO_2)_4$ and $K_3Fe(CN)_6$ (Strem Chemicals, Newburyport, MA).

Except where described below, current traces were filtered at 50 Hz (for single-channel currents) or 100 Hz (for macroscopic currents) using an 8-pole Bessel filter, digitized at 250 Hz–1 kHz and analyzed using pCLAMP9 software. Macroscopic current-voltage (I-V) relationships were constructed using depolarizing voltage ramp protocols (Linsdell & Hanrahan, 1996a, 1998). Background (leak) currents recorded before the addition of PKA were subtracted digitally, leaving uncontaminated CFTR currents (Linsdell & Hanrahan, 1998; Gong & Linsdell, 2003b).

The effects of intracellular channel blockers were compared under different steady-state, nonequilibrium ionic conditions. The relationship between macroscopic current inhibition and membrane voltage was routinely fitted by the simplest version of the Woodhull (1973) model of voltage-dependent block:

$$I/I_0 = K_i(V)/\{K_i(V) + [B]\} \quad (1)$$

where I is the current amplitude in the presence of the blocker B, I_0 is the control unblocked current amplitude and $K_i(V)$ is the voltage-dependent dissociation constant, the voltage dependence of which is given as follows:

$$K_i(V) = K_i(0)\ \exp\ (-z\delta VF/RT) \quad (2)$$

where $z\delta$ is the effective valence of the blocking ion (actual valence multiplied by the fraction of the transmembrane electric field apparently experienced during the blocking reaction) and F, R and T have their usual thermodynamic meanings.

Spectral analysis of macroscopic current variance was carried out on continuous current recordings at a membrane potential of −30 mV before and after addition of NPPB, as described previously (Gong et al., 2002b). Current recordings were filtered at 5 kHz, digitized at 10 kHz and then divided into nonoverlapping segments containing 8,192 data points (i.e., 819.2 ms/segment). Power density spectra were then calculated for each segment using BioPatch

Analysis software (BioLogic Science Instruments, Claix, France). Spectra from at least 100 segments were then averaged and fitted by the sum of two or three Lorentzian functions, as described in detail previously (Gong et al., 2002b). As in this previous study under similar conditions (Gong et al., 2002b), the dominant, low-frequency and low-amplitude, high-frequency Lorentzian components had corner frequencies in the range of 1–4 and 900–1,400 Hz, respectively; and these components were not significantly altered by the addition of NPPB to the intracellular solution.

Experiments were carried out at room temperature, 21–24°C. Values are given as mean ± standard error of the mean (SEM). Tests of statistical significance were carried out using a two-tailed *t*-test.

Results

Interaction between Internal and External $Pt(NO_2)_4^{2-}$ Ions

Block of CFTR Cl^- currents by intracellular $Pt(NO_2)_4^{2-}$ ions, as with many other open channel blockers of this channel, is weakened by permeant Cl^- ions in the extracellular solution (Gong & Linsdell, 2003b). To determine if impermeant $Pt(NO_2)_4^{2-}$ ions in the extracellular solution would mimic this effect of Cl^-, we investigated the block of macroscopic CFTR Cl^- currents in inside-out membrane patches by intracellular $Pt(NO_2)_4^{2-}$ (Fig. 1). To preclude the effects of Cl^- itself, these experiments were carried out using gluconate rather than Cl^- as the main extracellular anion. As shown in Figure 1*A*, inclusion of a low concentration of $K_2Pt(NO_2)_4$ in the extracellular solution weakened the blocking effects of intracellular $Pt(NO_2)_4^{2-}$. Under different steady-state conditions [with or without $Pt(NO_2)_4^{2-}$ in the extracellular solution], the voltage dependence of block by intracellular $Pt(NO_2)_4^{2-}$ was well described by a simple Woodhull model (Fig. 1*B*), as described previously under different ionic conditions (Gong & Linsdell, 2003b). Fits to equation 1 of data from individual patches indicate a $K_i(0)$ of 138 ± 12 μM (n = 5) without extracellular $Pt(NO_2)_4^{2-}$ compared to 518 ± 84 μM (n = 3) ($P < 0.001$) with 8 mM $Pt(NO_2)_4^{2-}$ in the extracellular solution. Thus, extracellular $Pt(NO_2)_4^{2-}$, like Cl^-, lowers the apparent affinity of block by intracellular $Pt(NO_2)_4^{2-}$ ions. However, extracellular Cl^- also increases the apparent voltage dependence of block by intracellular $Pt(NO_2)_4^{2-}$ (Gong & Linsdell, 2003b) and many other anionic blockers (McDonough et al., 1994; Sheppard & Robinson, 1997; Linsdell & Hanrahan, 1999; Gong & Linsdell, 2003a). In contrast, the Woodhull fits in Figure 1*B* suggest that extracellular $Pt(NO_2)_4^{2-}$ alters the affinity of block by intracellular $Pt(NO_2)_4^{2-}$ without significantly affecting the voltage dependence of block [$z\delta$ = -0.243 ± 0.025 (n = 5) without extracellular $Pt(NO_2)_4^{2-}$ and −0.184 ± 0.014 (n = 3) with 8 mM extracellular $Pt(NO_2)_4^{2-}$; $P > 0.1$].

The concentration-dependent effect of extracellular $Pt(NO_2)_4^{2-}$ on block by intracellular $Pt(NO_2)_4^{2-}$ is summarized in Figure 1*C,D*. Extracellular $Pt(NO_2)_4^{2-}$ caused a concentration-dependent increase in the apparent K_i for intracellular $Pt(NO_2)_4^{2-}$ (K_{IN}) both at 0 mV and at the recorded voltage at which block was strongest (−100 mV) (Fig. 1*C*) without significantly altering the apparent voltage dependence of the block (Fig. 1*D*).

To interpret the nature of the apparent interactions between intracellular and extracellular $Pt(NO_2)_4^{2-}$ ions, we need to know not only K_{IN} but also the affinity of extracellular $Pt(NO_2)_4^{2-}$ ions for the channel, K_{OUT}. Previously it was shown that extracellular $Pt(NO_2)_4^{2-}$ blocks CFTR with a much lower apparent affinity than intracellular $Pt(NO_2)_4^{2-}$ (Gong & Linsdell, 2003b); this is consistent with our ability to record macroscopic CFTR Cl^- currents with extracellular $Pt(NO_2)_4^{2-}$ concentrations as high as 8 mM (e.g., Fig. 1*A*). To characterize block by extracellular $Pt(NO_2)_4^{2-}$ ions under the same ionic conditions used in Figure 1, we recorded single-channel currents from inside-out membrane patches using pipette solutions containing gluconate plus varying concentrations of $Pt(NO_2)_4^{2-}$ (Fig. 2). As described previously using Cl^--containing extracellular solutions (Gong & Linsdell, 2003b), extracellular $Pt(NO_2)_4^{2-}$ caused a concentration-dependent decrease in apparent unitary current amplitude (Fig. 2*A,B*), consistent with a rapid open channel blocking effect. The concentration and voltage dependence of block is illustrated in Figure 2*C*. The straight-line fit to Figure 2*D* suggests a K_i of 2.30 mM at 0 mV and an effective valence, $z\delta$, of −0.611. This strong voltage dependence of block is consistent with inhibition being enhanced at positive voltages that would tend to draw anions into the pore from the extracellular solution.

The interaction between internal and external $Pt(NO_2)_4^{2-}$, illustrated in Figure 1*C*, is explored in more detail in Figure 3. The apparent affinity for internal $Pt(NO_2)_4^{2-}$, K_{IN}, is plotted as a function of external $Pt(NO_2)_4^{2-}$ concentration at −60 mV, a membrane potential at which both K_{IN} and K_{OUT} were determined directly. In Figure 3*A*, the solid line represents the expected relationship if internal and external $Pt(NO_2)_4^{2-}$ block the channel completely independently, while the dashed line is that if $Pt(NO_2)_4^{2-}$ bound at an external site excludes $Pt(NO_2)_4^{2-}$ from binding to an internal site:

$$K_{IN} = K_{IN}(0)\ \frac{K_{OUT} + [Pt(NO_2)_4]}{K_{OUT}} \qquad (3)$$

Clearly, neither of these scenarios is sufficient to explain quantitatively the interaction between internal and external $Pt(NO_2)_4^{2-}$ ions. Instead, it appears that the effect of external $Pt(NO_2)_4^{2-}$ on K_{IN} is

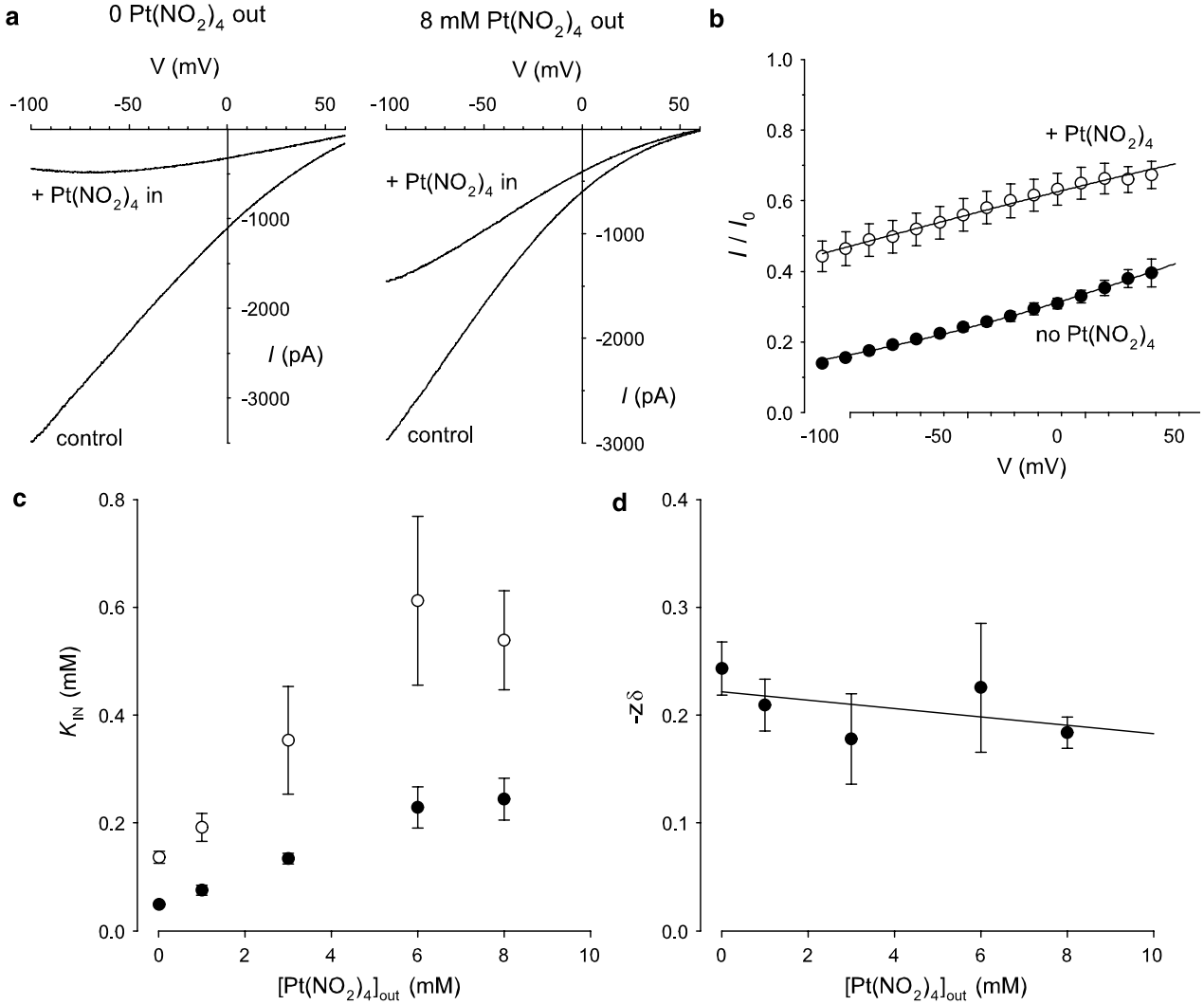

Fig. 1. Extracellular $Pt(NO_2)_4^{2-}$ modulates block by intracellular $Pt(NO_2)_4^{2-}$. (*A*) Example leak-subtracted macroscopic current-voltage relationships recorded from inside-out membrane patches following maximal channel activation with PKA followed by PPi, with either 0 or 8 mM $Pt(NO_2)_4^{2-}$ in the extracellular solution as indicated. In both cases, currents were recorded before (control) and after [+ $Pt(NO_2)_4$ in] addition of 300 μM $Pt(NO_2)_4^{2-}$ to the intracellular solution. (*B*) Mean fraction of control current remaining (I/I_0) following addition of 300 μM $Pt(NO_2)_4^{2-}$ to the intracellular solution either without or with 8 mM $Pt(NO_2)_4^{2-}$ in the extracellular solution. Mean of data from three to five patches fitted by equation 1 with $K_i(0)$ = 136 μM and $z\delta$ = −0.243 without extracellular $Pt(NO_2)_4^{2-}$ (●) and $K_i(0)$ = 500 μM and $z\delta$ = −0.182 with 8 mM extracellular $Pt(NO_2)_4^{2-}$ (○). (*C*) Mean apparent K_i for block by intracellular $Pt(NO_2)_4^{2-}$, K_{IN}, increases as a function of extracellular $Pt(NO_2)_4^{2-}$ concentration at representative voltages of 0 mV (○) and −100 mV (●). (*D*) Mean apparent voltage dependence of block by intracellular $Pt(NO_2)_4^{2-}$, $z\delta$, is independent of extracellular $Pt(NO_2)_4^{2-}$ concentration. Both (*C*) and (*D*) show the mean of data from three to five patches.

stronger than can be explained by a simple competitive interaction. To illustrate this point, the same data are fit in Figure 3*B* but this time allowing the value of K_{OUT} to vary. The best fit to equation 3 occurs when K_{OUT} = 1.97 mM. While this value has no physical meaning and does not correspond with any identifiable individual or aggregate effect of external $Pt(NO_2)_4^{2-}$ on the channel, the fact that it is so much lower than the observed K_{OUT} of 10.46 mM at −60 mV underlines the point that, for a competitive interaction to explain the effects of external $Pt(NO_2)_4^{2-}$ on channel block by internal $Pt(NO_2)_4^{2-}$, external $Pt(NO_2)_4^{2-}$ binding would need to be of much higher affinity than that estimated from external $Pt(NO_2)_4^{2-}$ inhibition of unitary Cl^- conductance. Similar discrepancies between the observed K_{OUT} and that necessary to model qualitatively the effects of external $Pt(NO_2)_4^{2-}$ on K_{IN} by a simple competitive mechanism were seen at other membrane potentials (*not shown*).

Since the measured K_{OUT} reflects $Pt(NO_2)_4^{2-}$ binding inside the pore where it interferes directly with Cl^- permeation, whereas the "modeled" K_{OUT} reflects interactions between $Pt(NO_2)_4^{2-}$ ions bound to the outside of the channel (but not necessarily within the pore) and blocking ions bound to the

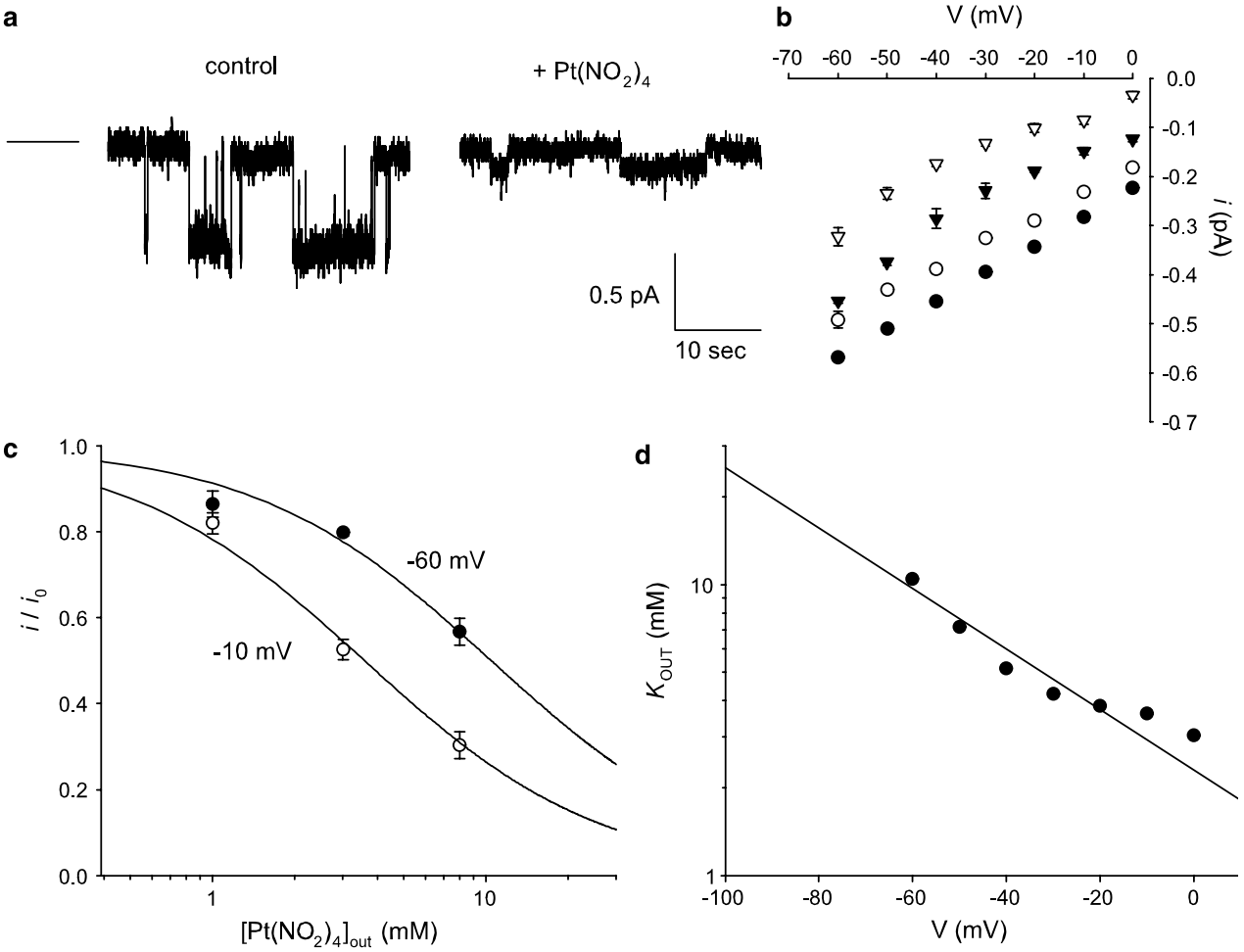

Fig. 2. Properties of block by extracellular $Pt(NO_2)_4^{2-}$. (*A*) Example single-channel currents recorded from inside-out membrane patches, following stimulation with PKA and ATP but in the absence of PPi, at −30 mV. These traces were recorded with no $Pt(NO_2)_4^{2-}$ (control) or with 8 mM $Pt(NO_2)_4^{2-}$ [+ $Pt(NO_2)_4$] in the extracellular solution. The closed-state current is indicated by the straight line to the far left. (*B*) Mean unitary current-voltage relationships recorded with different concentrations of $Pt(NO_2)_4^{2-}$ in the extracellular solution: 0 (●), 1 mM (○), 3 mM (▼), 8 mM (▽). Mean of data from three or four patches. (*C*) Mean fraction of control unitary current remaining (i/i_0) with different concentrations of $Pt(NO_2)_4^{2-}$ present in the extracellular solution, at membrane potentials of −60 mV (●) and −10 mV (○). The data have been fitted by the equation $i/i_0 = 1/[1+([Pt(NO_2)_4^{2-}]/K_{OUT})]$ to estimate the apparent affinity of the blocking reaction by extracellular $Pt(NO_2)_4^{2-}$, K_{OUT}. The fits shown suggest K_{OUT} = 10.46 mM at −60 mV and 3.60 mM at −10 mV. (*D*) Similar analysis at other membrane potentials reveals a steep voltage dependence of block; the fitted straight line suggests $z\delta = -0.611$ according to equation 2.

inside of the channel, we will use this discrepancy between K_{OUT} values to argue for the existence of an additional, non-pore binding site for external $Pt(NO_2)_4^{2-}$ ions (*see* Discussion).

Interactions between Pt $(NO_2)_4^{2-}$ and Other Blockers

The ability of extracellular Cl^- ions to weaken the apparent affinity of intracellular open channel blockers is common to many large blocking molecules (*see* Introduction). To determine if extracellular $Pt(NO_2)_4^{2-}$ ions could also affect block by large intracellular organic anions, we investigated two well-known CFTR blockers, glibenclamide (Sheppard & Robinson, 1997; Zhang, Zeltwanger & McCarty, 2004) and NPPB (Zhang, Zeltwanger & McCarty, 2000). These are both quite large blocker molecules (molecular weights 494 and 300, respectively), and we presume that, like $Pt(NO_2)_4^{2-}$, they are not capable of passing through the CFTR channel.

Under low external Cl^- ionic conditions, addition of 8 mM $Pt(NO_2)_4^{2-}$ to the extracellular solution did indeed weaken the blocking effects of both glibenclamide (Fig. 4*A,B*) and NPPB (Fig. 4*C,D*). For glibenclamide, fits of data from individual patches to equation 1 indicate a $K_i(0)$ of 17.6 ± 1.9 μM for control (n = 3), increasing significantly to 54.3 ± 4.9 μM with 8 mM $Pt(NO_2)_4^{2-}$ (n = 3) ($P < 0.0025$); however, as with intracellular $Pt(NO_2)_4^{2-}$, there was no change

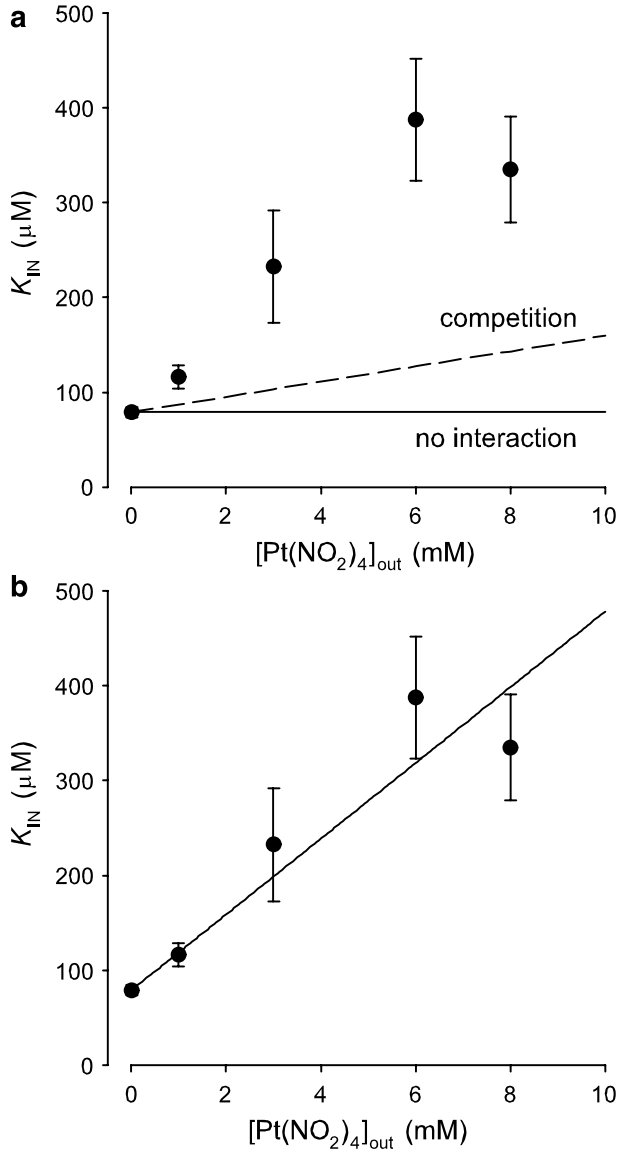

Fig. 3. Qualitative analysis of the interaction between extracellular and intracellular $Pt(NO_2)_4^{2-}$. Both panels show the same data, the dependence of K_{IN} on extracellular $Pt(NO_2)_4^{2-}$ concentration at −60 mV (*see* Fig. 1*C* for similar data at other membrane potentials). (*A*) Predictions of simple models whereby internal and external $Pt(NO_2)_4^{2-}$ inhibit the channel independently (*solid line*) or compete for binding inside the channel (*dashed line*, *see* equation 3). (*B*) Fit of the data with simple competition between internal and external $Pt(NO_2)_4^{2-}$. The fit to equation 3 gives an apparent K_{OUT} of 1.97 mM, in conflict with the observed K_{OUT} of 10.46 mM at this voltage.

in the apparent voltage dependence of glibenclamide block [$z\delta = -0.314 \pm 0.013$ in control ($n = 3$), -0.252 ± 0.036 with 8 mM $Pt(NO_2)_4^{2-}$ ($n = 3$); $P > 0.1$]. For NPPB, $K_i(0)$ increased from 56.5 ± 2.0 μM for control ($n = 3$) to 81.2 ± 7.6 μM with 8 mM $Pt(NO_2)_4^{2-}$ ($n = 4$) ($P < 0.05$), again with no significant changes in voltage dependence of block [$z\delta = -0.312 \pm 0.017$ in control ($n = 3$), -0.259 ± 0.048 with 8 mM $Pt(NO_2)_4^{2-}$ ($n = 4$); $P > 0.1$].

If extracellular anions bind within the channel permeation pathway to interact electrostatically with bound intracellular anions and destabilize their binding, then we would expect an effect of extracellular anions predominantly on the off-rate of the intracellular blocking molecule. To gain some information on the on- and off-rates for intracellular blockers under different ionic conditions, we used spectral analysis of macroscopic currents (Venglarik et al., 1996; Gong et al., 2002b; Scott-Ward et al., 2004) (*see* Methods). Unfortunately, we found no measurable increase in current variance over the frequency range investigated (1–4,096 Hz) associated with macroscopic current block by either $Pt(NO_2)_4^{2-}$ (perhaps because the blocking reaction is too fast) or glibenclamide (probably because the blocking reaction is too slow; *see* Schultz et al., 1996). However, at −30 mV membrane potential, NPPB led to the introduction of a new component of current variance at intermediate frequencies (50–300 Hz) (Fig. 5*A*). The frequency of NPPB-induced current variance was estimated by fitting spectra such as those shown in Figure 5*A* with the sum of two (in control) or three (with NPPB) Lorentzian functions (*see* Methods). Both with and without 8 mM $Pt(NO_2)_4^{2-}$ in the extracellular solution, the corner frequency of the NPPB-induced, intermediate frequency Lorentzian component (f_c) increased with increasing NPPB concentration (Fig. 5*B*). As described previously (Venglarik et al., 1996; Gong et al., 2002b; Scott-Ward et al., 2004), blocker-dependent changes in f_c were used to estimate blocker on- and off-rates, k_{on} and k_{off}, according to a simple kinetic scheme:

$$\text{Closed} \underset{k_{close}}{\overset{k_{open}}{\rightleftarrows}} \text{Open} \underset{k_{off}}{\overset{k_{on}}{\rightleftarrows}} \text{Blocked}$$

Such a scheme predicts that $2\pi f_c$ will be a linear function of blocker concentration with an intercept of k_{off} and a slope of k_{on} (Lindemann & van Driessche, 1977; Venglarik et al., 1996). Such a relationship is shown in Figure 5*B*. Unfortunately, NPPB could not be studied over the same concentration range with and without $Pt(NO_2)_4^{2-}$ in the pipette solution since without external $Pt(NO_2)_4^{2-}$ high concentrations of NPPB caused almost total inhibition of the current, while with external $Pt(NO_2)_4^{2-}$ low concentrations of NPPB caused weak block with no discernible increase in current variance. As shown in Figure 5*B*, in the absence of $Pt(NO_2)_4^{2-}$, the data are well fitted by a straight line, giving a k_{on} of 10.3 μM^{-1} s^{-1} and a k_{off} of 273 s^{-1}; the ratio of these two rates, k_{off}/k_{on}, suggests a K_d of 26.5 μM (at −30 mV). With 8 mM external $Pt(NO_2)_4^{2-}$, the data were considerably less well fitted, with the straight-line fit shown in Figure 5*B*

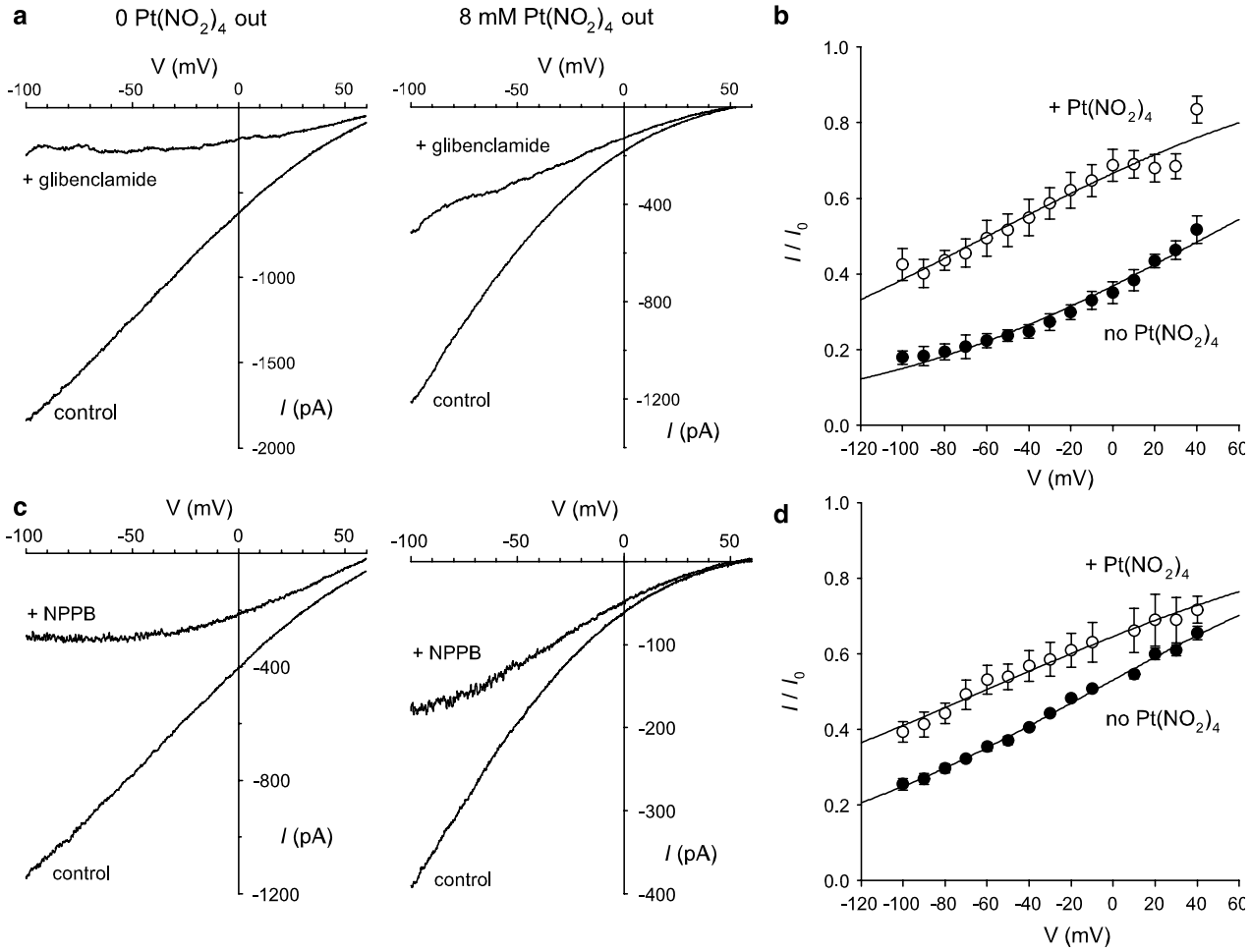

Fig. 4. Interaction between extracellular $Pt(NO_2)_4^{2-}$ and intracellular blockers glibenclamide and NPPB. (*A*, *C*) Example macroscopic current-voltage relationships recorded with either 0 or 8 mM $Pt(NO_2)_4^{2-}$ in the extracellular solution, before (control) and after addition of either 30 μM glibenclamide (*A*, + glibenclamide) or 50 μM NPPB (*C*, + NPPB) to the intracellular solution. (*B*, *D*) Mean fraction of control current remaining (I/I_0) following addition of either 30 μM glibenclamide (*B*) or 50 μM NPPB (*D*) to the intracellular solution. In both cases, experiments were carried out either without (●) or with (○) 8 mM $Pt(NO_2)_4^{2-}$ in the extracellular solution. Mean of data from three to five patches fitted by equation 1 in both (*B*) and (*D*). In (*B*), the fit gives $K_i(0)$ = 17.5 μM and $z\delta$ = -0.304 without extracellular $Pt(NO_2)_4^{2-}$ (●) and $K_i(0)$ = 59.8 μM and $z\delta$ = −0.295 with 8 mM extracellular $Pt(NO_2)_4^{2-}$ (○). In (*D*), the fit gives $K_i(0)$ = 56.5 μM and $z\delta$ = −0.312 without extracellular $Pt(NO_2)_4^{2-}$ (●) and $K_i(0)$ = 91.0 μM and $z\delta$ = −0.246 with 8 mM extracellular $Pt(NO_2)_4^{2-}$ (○).

suggesting a k_{on} of 6.79 μM^{-1} s^{-1} and a k_{off} of 337 s^{-1}, giving a K_d of 49.6 μM. Both these K_d values are in good agreement with K_i values estimated by macroscopic I-V curve analysis (*see* Fig. 4*C*,*D*).

These results suggest that extracellular $Pt(NO_2)_4^{2-}$ causes a 34% decrease in NPPB on-rate and a 23% increase in NPPB off-rate. However, it is difficult to know how significant these apparent changes in blocker on- and off-rates are. The straight-line fit to the data in the presence of extracellular $Pt(NO_2)_4^{2-}$ shown in Figure 5*B* is considerably less convincing than that in the absence of $Pt(NO_2)_4^{2-}$. In particular, since the blocker off-rate is determined by the extrapolated *x*-intercept of this straight line, a small change in the form of the fit could result in a significant change in apparent NPPB off-rate. Importantly, at no NPPB concentration was the apparent f_c greater in the presence of extracellular $Pt(NO_2)_4^{2-}$ than in its absence (Fig. 5*B*), questioning the validity of a higher estimated blocker off-rate in the presence of $Pt(NO_2)_4^{2-}$. Therefore, while unbiased inspection of the results from Figure 5*B* suggests that extracellular $Pt(NO_2)_4^{2-}$ decreases the on-rate for block by intracellular NPPB and at the same time increases its off-rate, we are unable to ascribe a level of significance to these results. Perhaps the most conservative interpretation of these data is that the effects of extracellular $Pt(NO_2)_4^{2-}$ do not appear consistent with a simple knock-off mechanism whereby $Pt(NO_2)_4^{2-}$ predominantly affects blocker off-rate.

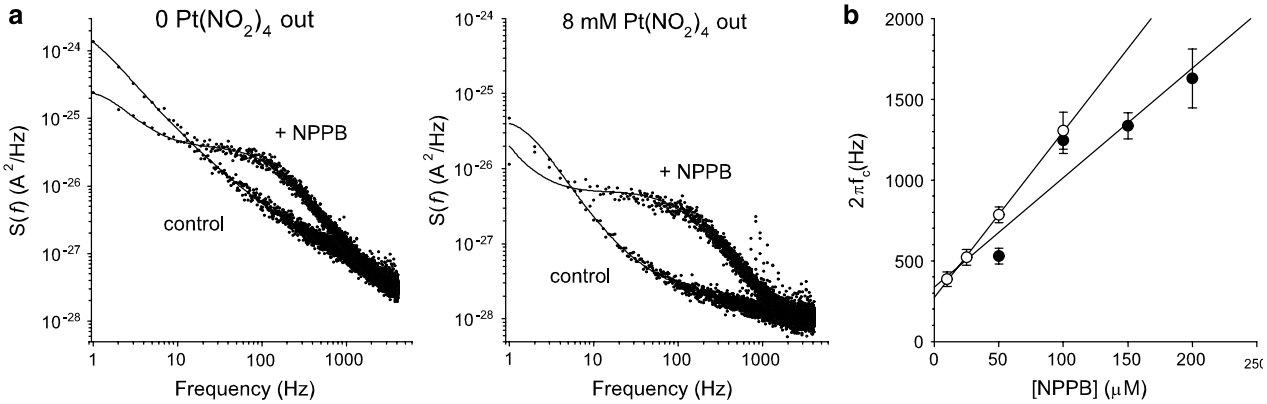

Fig. 5. Spectral analysis of the sensitivity of NPPB block to extracellular $Pt(NO_2)_4^{2-}$. (*A*) Power spectra calculated for macroscopic CFTR currents in inside-out membrane patches at −30 mV before (control) and after (+ NPPB) addition of 100 μM NPPB to the intracellular solution. These spectra come from currents recorded with either 0 or 8 mM $Pt(NO_2)_4^{2-}$ in the extracellular solution as indicated. Spectra have been fitted by the sum of two (control) or three (+ NPPB) Lorentzian functions of the form $S_f = S_0 / (1+(f/f_c)^2)$, where S_f is the current variance per unit frequency at each frequency f, S_0 is the maximum value of S as f approaches zero and f_c is the corner frequency at which $S_f = S_0/2$ (*see* Gong et al., 2002b). (*B*) Dependence of f_c of the intermediate-frequency Lorentzian component associated with NPPB block on blocker concentration, estimated either without (○) or with (●) 8 mM $Pt(NO_2)_4^{2-}$ in the extracellular solution. Mean of data from three or four patches. The fitted straight lines have an intercept of 273 Hz and a slope of 10.3 Hz μM^{-1} without $Pt(NO_2)_4^{2-}$ and an intercept of 337 Hz and a slope of 6.79 Hz μM^{-1} with 8 mM $Pt(NO_2)_4^{2-}$.

Effects of External $Fe(CN)_6^{3-}$

The analysis of the interaction between intracellular and extracellular $Pt(NO_2)_4^{2-}$ summarized in Figure 3 suggests that the ability of extracellular $Pt(NO_2)_4^{2-}$ to affect block by intracellular $Pt(NO_2)_4^{2-}$ cannot be explained solely by the observed effect of extracellular $Pt(NO_2)_4^{2-}$ ions entering the permeation pathway to block Cl^- current. To further explore the possibility that external anions could interact with internal blocking anions without entering deeply into the pore, we looked for multivalent anions that did not block Cl^- permeation when present in the extracellular solution. One such anion was the trivalent $Fe(CN)_6^{3-}$, which at external concentrations as high as 5 mM had no significant effect on unitary current amplitude (Fig. 6*A,B*). In spite of this apparent inability to enter far enough into the pore from the extracellular solution to have any impact on Cl^- permeation, external $Fe(CN)_6^{3-}$ did significantly affect block by intracellular $Pt(NO_2)_4^{2-}$ ions (Fig. 6*C*). Indeed, fits to data from individual patches with equation 1 suggested that 5 mM $Fe(CN)_6^{3-}$ increased the $K_i(0)$ for block by intracellular $Pt(NO_2)_4^{2-}$ from 138 ± 12 μM (n = 5) to 286 ± 45 μM (n = 3) ($P < 0.01$). As with external $Pt(NO_2)_4^{2-}$, this effect of external $Fe(CN)_6^{3-}$ was not associated with any change in apparent blocker voltage dependence [$z\delta$ for intracellular $Pt(NO_2)_4^{2-}$ was –0.243 ± 0.025 (n = 5) for control and –0.311 ± 0.028 (n = 3) with $Fe(CN)_6^{3-}$; $P > 0.1$]. One surprising prediction of these results is that, in the presence of intracellular $Pt(NO_2)_4^{2-}$ ions, addition of $Fe(CN)_6^{3-}$ to the extracellular solution should slightly increase unitary current amplitude; however, this prediction was not tested directly.

Discussion

Weakening of the inhibitory effects of intracellular open channel blockers of CFTR by extracellular Cl^- ions is a commonly observed phenomenon (McDonough et al., 1994; Linsdell & Hanrahan, 1996b, 1999; Sheppard & Robinson, 1997; Gong et al., 2002b; Zhou et al., 2002; Gong & Linsdell, 2003b) that has previously been used as diagnostic of an open channel block mechanism (Linsdell & Gong, 2002; Cai et al., 2004). We found that low concentrations of the impermeant anion $Pt(NO_2)_4^{2-}$ in the extracellular solution also significantly weakened the blocking effects of three different intracellular open channel blockers: $Pt(NO_2)_4^{2-}$, glibenclamide and NPPB. Assuming that none of these substances is capable of passing through the pore, this suggests that binding of $Pt(NO_2)_4^{2-}$ to an extracellularly accessible site weakens the binding of $Pt(NO_2)_4^{2-}$, glibenclamide and NPPB to a separate, intracellularly accessible site or sites.

The usual interpretation of the effects of external Cl^- on internal blockers – related to the classical "knock-off" effect – is illustrated schematically in Figure 7*A*. It is assumed that Cl^- entering the pore from the outside will bind close to bound blocking ions and repel them electrostatically, pushing them back into the cytoplasmic solution and decreasing their apparent affinity by increasing blocker off-rate (McDonough et al., 1994; Linsdell et al., 1997; Zhou et al., 2002; Gong & Linsdell, 2003a). However, several lines of evidence argue against such a mechanism of action for external $Pt(NO_2)_4^{2-}$ ions: (1) the interaction between external and internal $Pt(NO_2)_4^{2-}$ ions appears to be too strong to be accounted for by

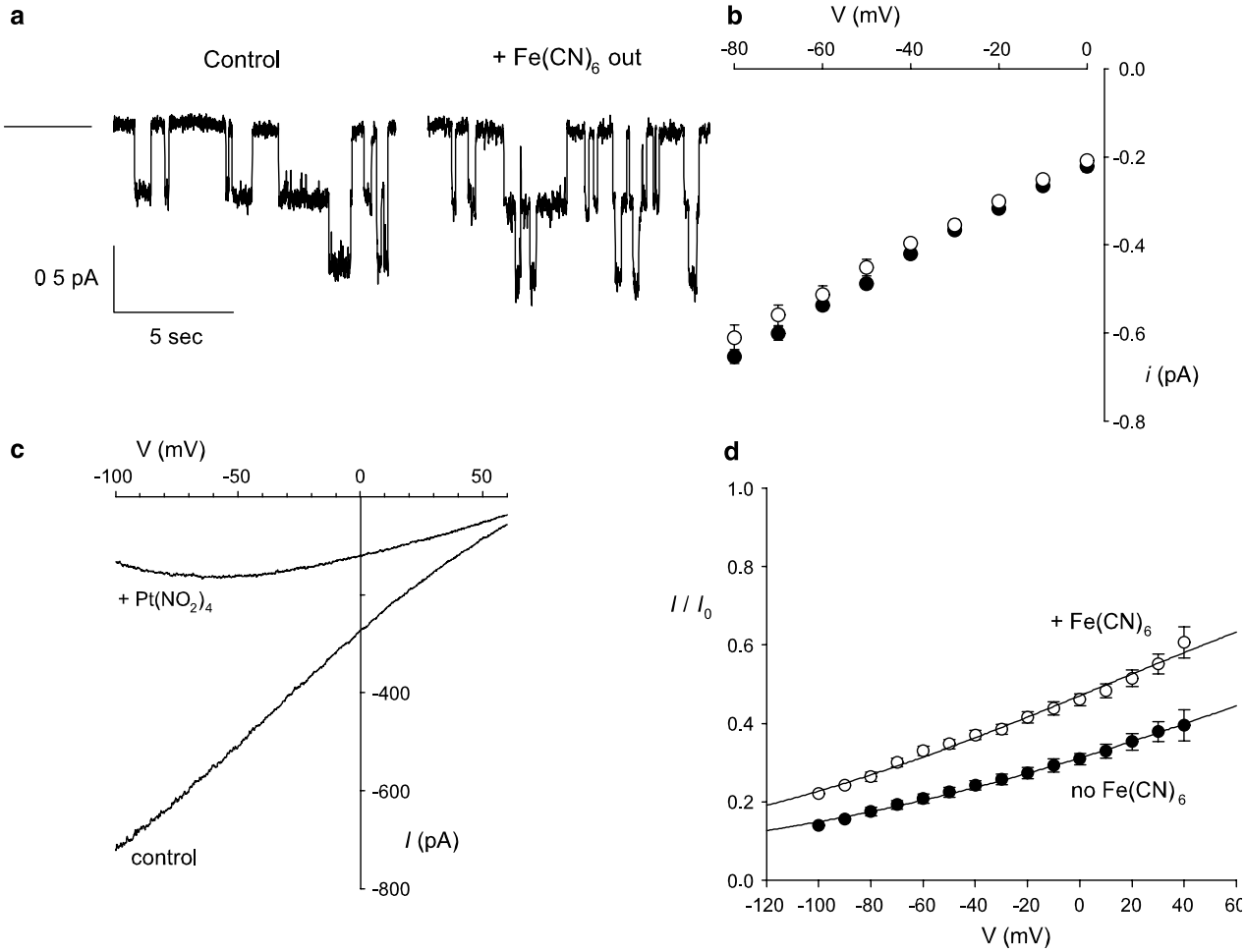

Fig. 6. Interaction between extracellular $Fe(CN)_6^{3-}$ and intracellular $Pt(NO_2)_4^{2-}$. (*A*) Example single-channel currents recorded from inside-out membrane patches at –60 mV, with no $Fe(CN)_6^{3-}$ (control) or with 5 mM $Fe(CN)_6^{3-}$ [+ $Fe(CN)_6$] in the extracellular solution. The closed-state current is indicated by the straight line to the far left. (*B*) Mean unitary current-voltage relationships recorded under these conditions, for control (●) or 5 mM $Fe(CN)_6^{3-}$ (○). Mean of data from four or five patches. There was no significant difference in mean unitary current amplitude at any membrane potential examined. (*C*) Example macroscopic current-voltage relationships recorded with 5 mM $Fe(CN)_6^{3-}$ in the extracellular solution, before (control) and after addition of 300 μM $Pt(NO_2)_4^{2-}$ [+$Pt(NO_2)_4$] to the intracellular solution. (*D*) Comparison of the mean blocking effects of 300 μM $Pt(NO_2)_4^{2-}$ under these conditions (○) to those without $Fe(CN)_6^{3-}$ in the extracellular solution (●; see Fig. 1*A, B*). Mean of data from three to five patches fitted by equation 1 with $K_i(0)$ = 136 μM and $z\delta$ = −0.243 without extracellular $Fe(CN)_6^{3-}$ (●) and $K_i(0)$ = 267 μM and $z\delta$ = −0.282 with 5 mM extracellular $Fe(CN)_6^{3-}$ (○).

models in which ions compete directly or indirectly for binding sites inside the pore (Fig. 3); (2) the effects of external $Pt(NO_2)_4^{2-}$ ions are reproduced by $Fe(CN)_6^{3-}$ ions, which do not appear to enter the pore at all (Fig. 6); (3) external $Pt(NO_2)_4^{2-}$ ions reduce the affinity of intracellular blockers without altering their voltage dependence (Figs. 1*D*, 4*B* and *D*), even though entry of $Pt(NO_2)_4^{2-}$ ions into the pore appears to be strongly voltage-dependent (Fig. 2*D*), and in contrast with external Cl^- ions which reduce blocker affinity and at the same time increase blocker voltage dependence (McDonough et al., 1994; Sheppard & Robinson, 1997; Linsdell & Hanrahan, 1999; Gong & Linsdell, 2003a,b); (4) the interaction between external $Pt(NO_2)_4^{2-}$ ions and internal NPPB does not appear to reflect predominantly or exclusively an increase in the off-rate for this blocker (Fig. 5).

The strong effects of extracellular $Pt(NO_2)_4^{2-}$ ions on intracellular blockers, together with the finding that extracellular $Fe(CN)_6^{3-}$ can interact with intracellular blocking ions without apparently entering into the pore, are more consistent with a model in which external ions act at a site away from the pore itself to destabilize intracellular blockers. Such a model is proposed schematically in Figure 7*B*. Anions such as $Pt(NO_2)_4^{2-}$ and $Fe(CN)_6^{3-}$ bind to a site (or sites) on the extracellular face of the channel but outside of the pore such that binding here does not directly influence Cl^- movement through the pore.

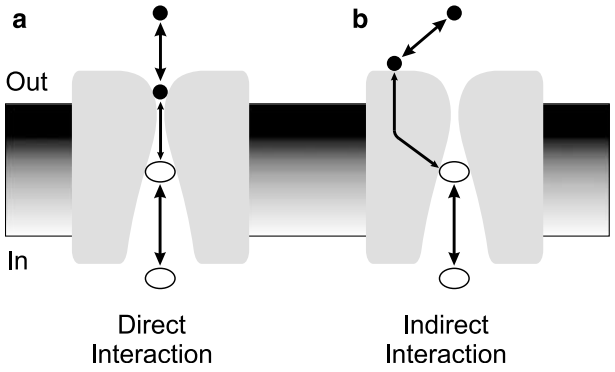

Fig. 7. Direct and indirect interactions between extracellular and intracellular anions. (*A*) Conventional direct interaction between an extracellular anion (*black*) and intracellular blocking anion (*white*). External anions enter the pore and bind to a site extracellular to the blocker binding site; electrostatic repulsion between the two bound anions then accelerates their exit from the pore. This leads to an increase in the blocker off-rate and a consequent decrease in its overall affinity. (*B*) We propose that extracellular anions such as $Pt(NO_2)_4^{2-}$ and $Fe(CN)_6^{3-}$ can destabilize blocker binding indirectly without entering the pore. In this model, external anion binding causes a conformational change in the pore, lowering the affinity of intracellular blocker interactions at a distant binding site.

However, anion binding to this site causes a conformational change in the channel protein, which alters the structure of the inner pore, altering access and/or stability of intracellular anions at a cytoplasmic blocker binding site. As a result, external anion binding outside the pore weakens binding of intracellular blocking ions inside the pore. This kind of mechanism has precedent in other channel types. For example, the sensitivity of TEA block of K^+ channel pores to ionic conditions has been proposed to result from permeant ion binding that causes a conformational change in the TEA binding site (Immke et al., 1999; Spassova & Lu, 1999). From our present results we cannot tell if $Pt(NO_2)_4^{2-}$ and $Fe(CN)_6^{3-}$ bind to a specific site on the extracellular face of the channel or if they act by screening one or more positive extracellular surface charges. In either case, the effects of these extracellular anions would be to cause a conformational change at some distance from their extracellular site of action.

The model shown in Figure 7*B* is able to explain the discrepancy between observed and "estimated" affinities for external $Pt(NO_2)_4^{2-}$ (K_{OUT} in Fig. 3). Thus, the observed K_{OUT} reflects only $Pt(NO_2)_4^{2-}$ binding within the pore (Fig. 7*A*), whereas the "estimated" K_{OUT} required to model the effects of external $Pt(NO_2)_4^{2-}$ on K_{IN} could reflect extracellular $Pt(NO_2)_4^{2-}$ binding in the pore (Fig. 7*A*), outside the pore (Fig. 7*B*) or some combination of both. In fact, binding of $Pt(NO_2)_4^{2-}$ [or $Fe(CN)_6^{3-}$] to the extra-pore site shown in Figure 7*B* is expected to alter K_{IN} but not K_{OUT}. Furthermore, whereas extracellular $Pt(NO_2)_4^{2-}$ entry into the pore appears to be strongly voltage-dependent (Fig. 2*D*), the extra-pore site may be outside of the transmembrane electric field, allowing anion binding to affect blocker binding in a voltage-independent manner.

The effects of extracellular $Pt(NO_2)_4^{2-}$ on intracellular blocker affinity but not voltage dependence are reminiscent of those of some other extracellular anions on CFTR open channel block by intracellular $Au(CN)_2^-$ ions (Gong & Linsdell, 2003a). In this case, while Cl^- and other anions showing high permeability in CFTR affected both the affinity and voltage dependence of block, anions with low permeability could weaken block by intracellular $Au(CN)_2^-$ but did not result in strong blocker voltage dependence, as seen with extracellular Cl^- (Gong & Linsdell, 2003a). Thus, it may be that extracellular anions show different interactions with intracellular blocking ions depending on whether these extracellular anions are permeant (like Cl^-) or impermeant [like $Pt(NO_2)_4^{2-}$]. One possible scenario is that impermeant anions like $Pt(NO_2)_4^{2-}$ bind to an extracellular site on the channel to weaken the blocking effects of intracellular anions by a nonelectrostatic mechanism (Fig. 7*B*), whereas permeant anions like Cl^- are able to travel further into the pore from the extracellular solution, to a site at which they are able to interact with intracellular blockers in a way that affects both their affinity and their voltage dependence (Fig. 7*A*). These effects could in theory result from either electrostatic or nonelectrostatic interactions. In addition, we cannot rule out the possibility that much of the effect of extracellular Cl^- on the apparent affinity of intracellular blockers results from interactions with the extra-pore anion binding site suggested in Figure 7*B*.

Extracellular anions have recently been shown to affect both the gating (Wright et al., 2004) and the ionic selectivity (Shcheynikov et al., 2004) of CFTR. In both these cases, it was suggested that binding of anions to an extracellularly accessible site on the channel would lead to a conformational change in the channel protein sufficient to affect intracellular processes. Indeed, a different pattern of tryptic digest of the CFTR protein is observed in Cl^--containing *vs.* Cl^--free media, suggesting that Cl^- binding controls a discrete conformational switch in CFTR (Shcheynikov et al., 2004). Thus the ionic composition of the extracellular solution may be an important factor regulating CFTR structure and activity. Whether the diverse effects of extracellular anions on CFTR functional properties (intracellular blocker binding, channel gating, ionic selectivity) reflect anion binding to a common or different extracellular binding sites will be an important question for future studies. Our present results suggest that anions present in the extracellular solution have access to binding sites both within and outside of the channel permeation pathway and that binding to either of these sites can

influence the functional properties of the pore. We further suggest that external $Pt(NO_2)_4^{2-}$ and $Fe(CN)_6^{3-}$ represent good probes of an extracellular anion binding site located outside of the pore (as proposed in Fig. 7*B*) that could be used in combination with site-directed mutagenesis studies to identify the molecular determinants of this site. Future molecular identification of this site would allow us to address the question of whether binding of Cl^- and/or other physiologically relevant anions (such as HCO_3^-) to this site affects the normal physiological function of CFTR.

We thank Chantal St. Aubin for providing the single-channel data shown in Figure 6*A* and Kellie Davis and Jeremy Roy for technical assistance. This work was supported by the Canadian Institutes of Health Research.

References

Cai, Z., Scott-Ward, T.S., Li, H., Schmidt, A., Sheppard, D.N. 2004. Strategies to investigate the mechanism of action of CFTR modulators. *J. Cyst. Fibros.* **3(Suppl.2):**141–147

Chang, X.-B., Kartner, N., Seibert, F.S., Aleksandrov, A.A., Kloser, A.W., Kiser, G., Riordan, J.R. 1998. Heterologous expression systems for study of cystic fibrosis transmembrane conductance regulator. *Methods Enzymol.* **292:**616–629

Cohen, J., Schulten, K. 2004. Mechanism of anionic conduction across ClC. *Biophys. J.* **86:**836–845

Doyle, D.A., Cabral, J.M., Pfuetzner, R.A., Kuo, A., Gulbis, J.M., Cohen, S.L., Chait, B.T., MacKinnon, R. 1998. The structure of the potassium channel: Molecular basis of K^+ conduction and selectivity. *Science* **280:**69–77

Dutzler, R., Campbell, E.B., MacKinnon, R. 2003. Gating the selectivity filter in ClC chloride channels. *Science* **300:**108–112

Ge, N., Muise, C.N., Gong, X., Linsdell, P. 2004. Direct comparison of the functional roles played by different transmembrane regions in the cystic fibrosis transmembrane conductance regulator chloride channel pore. *J. Biol. Chem.* **279:**55283–55289

Gong, X., Burbridge, S.M., Cowley, E.A., Linsdell, P. 2002a. Molecular determinants of $Au(CN)_2^-$ binding and permeability within the cystic fibrosis transmembrane conductance regulator Cl^- channel pore. *J. Physiol.* **540:**39–47

Gong, X., Burbridge, S.M., Lewis, A.C., Wong, P.Y.D., Linsdell, P. 2002b. Mechanism of lonidamine inhibition of the CFTR chloride channel. *Br. J. Pharmacol.* **137:**928–936

Gong, X., Linsdell, P. 2003a. Coupled movement of permeant and blocking ions in the CFTR chloride channel pore. *J. Physiol.* **549:**375–385

Gong, X., Linsdell, P. 2003b. Mutation-induced blocker permeability and multiion block of the CFTR chloride channel pore. *J. Gen. Physiol.* **122:**673–687

Gupta, J., Linsdell, P. 2002. Point mutations in the pore region directly or indirectly affect glibenclamide block of the CFTR chloride channel. *Pfluegers Arch.* **443:**739–747

Hille, B. 2001. Ion Channels of Excitable Membranes. Sinauer Associates, Sunderland, MA

Immke, D., Wood, M., Kiss, L., Korn, S.J. 1999. Potassium-dependent changes in the conformation of the Kv2.1 potassium channel pore. *J. Gen. Physiol.* **113:**819–836

Lindemann, B., Driessche, W. 1977. Sodium-specific membrane channels of frog skin are pores: Current fluctuations reveal high turnover. *Science* **195:**292–294

Linsdell, P. 2005. Location of a common inhibitor binding site in the cytoplasmic vestibule of the cystic fibrosis transmembrane conductance regulator chloride channel pore. *J. Biol. Chem.* **280:**8945–8950

Linsdell, P. 2006. Mechanism of chloride permeation in the cystic fibrosis transmembrane conductance regulator chloride channel. *Exp. Physiol.* **91:**123–129

Linsdell, P., Gong, X. 2002. Multiple inhibitory effects of $Au(CN)_2^-$ ions on cystic fibrosis transmembrane conductance regulator Cl^- channel currents. *J. Physiol.* **540:**29–39

Linsdell, P., Hanrahan, J.W. 1996a. Disulphonic stilbene block of cystic fibrosis transmembrane conductance regulator Cl^- channels expressed in a mammalian cell line and its regulation by a critical pore residue. *J. Physiol.* **496:**687–693

Linsdell, P., Hanrahan, J.W. 1996b. Flickery block of single CFTR chloride channels by intracellular anions and osmolytes. *Am. J. Physiol. Cell Physiol.* **271:**C628–C634

Linsdell, P., Hanrahan, J.W. 1998. Adenosine triphosphate-dependent asymmetry of anion permeation in the cystic fibrosis transmembrane conductance regulator chloride channel. *J. Gen. Physiol.* **111:**601–614

Linsdell, P., Hanrahan, J.W. 1999. Substrates of multidrug resistance-associated proteins block the cystic fibrosis transmembrane conductance regulator chloride channel. *Br. J. Pharmacol.* **126:**1471–1477

Linsdell, P., Tabcharani, J.A., Hanrahan, J.W. 1997. Multi-ion mechanism for ion permeation and block in the cystic fibrosis transmembrane conductance regulator chloride channel. *J. Gen. Physiol.* **110:**365–377

MacKinnon, R. 2003. Potassium channels. *FEBS Lett.* **555:**62–65

MacKinnon, R., Miller, C. 1988. Mechanism of charybdotoxin block of the high-conductance, Ca^{2+}-activated K^+ channel. *J. Gen. Physiol.* **91:**335–349

McDonough, S., Davidson, N., Lester, H.A., McCarty, N.A. 1994. Novel pore-lining residues in CFTR that govern permeation and open-channel block. *Neuron* **13:**623–634

Newland, C.F., Adelman, J.P., Tempel, B.L., Almers, W. 1992. Repulsion between tetraethylammonium ions in cloned voltage-gated potassium channels. *Neuron* **8:**975–982

Neyton, J., Miller, C. 1988. Discrete Ba^{2+} block as a probe of ion occupancy and pore structure in the high-conductance Ca^{2+}-activated K^+ channel. *J. Gen. Physiol.* **92:**569–586

Sather, W.A., McCleskey, E.W. 2003. Permeation and selectivity in calcium channels. *Annu. Rev. Physiol.* **65:**133–159

Schultz, B.D., DeRoos, A.D.G., Venglarik, C.J., Singh, A.K., Frizzell, R.A., Bridges, R.J. 1996. Glibenclamide blockade of CFTR chloride channels. *Am. J. Physiol. Lung Cell Mol. Physiol.* **271:**L192–L200

Scott-Ward, T.S., Li, H., Schmidt, A., Cai, Z., Sheppard, D.N. 2004. Direct block of the cystic fibrosis transmembrane conductance regulator Cl^- channel by niflumic acid. *Mol. Membr. Biol.* **21:**27–38

Shcheynikov, N., Kim, K.H., Kim, K., Dorwart, M.R., Ko, S.B.H., Goto, H., Naruse, S., Thomas, P.J., Muallem, S. 2004. Dynamic control of cystic fibrosis transmembrane conductance regulator Cl^-/HCO_3^- selectivity by external Cl^-. *J. Biol. Chem.* **279:**21857–21865

Sheppard, D.N., Robinson, K.A. 1997. Mechanism of glibenclamide inhibition of cystic fibrosis transmembrane conductance regulator Cl^- channels expressed in a murine cell line. *J. Physiol.* **503:**333–346

Spassova, M., Lu, Z. 1999. Tuning the voltage dependence of tetraethylammonium block with permeant ions in an inward-rectifier K^+ channel. *J. Gen. Physiol.* **114:**415–426

Thompson, J., Begenisich, T. 2000. Interaction between quaternary ammonium ions in the pore of potassium channels. Evidence against an electrostatic repulsion mechanism. *J. Gen. Physiol.* **115:**769–782

Venglarik, C.J., Schultz, B.D., DeRoos, A.D.G., Singh, A.K., Bridges, R.J. 1996. Tolbutamide causes open channel blockade of cystic fibrosis transmembrane conductance regulator Cl^- channels. *Biophys. J.* **70:**2696–2703

Woodhull, A.M. 1973. Ionic blockage of sodium channels in nerve. *J. Gen. Physiol.* **61:**687–708

Wright, A.M., Gong, X., Verdon, B., Linsdell, P., Mehta, A., Riordan, J.R., Argent, B.E., Gray, M.A. 2004. Novel regulation of cystic fibrosis transmembrane conductance regulator (CFTR) channel gating by external chloride. *J. Biol. Chem.* **279:**41658–41663

Zhang, Z.-R., Zeltwanger, S., McCarty, N.A. 2000. Direct comparison of NPPB and DPC as probes of CFTR expressed in *Xenopus* oocytes. *J. Membr. Biol.* **175:**35–52

Zhang, Z.-R., Zeltwanger, S., McCarty, N.A. 2004. Steady-state interactions of glibenclamide with CFTR: Evidence for multiple sites in the pore. *J. Membr. Biol.* **199:**15–28

Zhou, Z., Hu, S., Hwang, T.-C. 2001a. Voltage-dependent flickery block of an open cystic fibrosis transmembrane conductance regulator (CFTR) channel pore. *J. Gen. Physiol.* **532:**435–448

Zhou, Z., Hu, S., Hwang, T.-C. 2002. Probing an open CFTR pore with organic anion blockers. *J. Gen. Physiol.* **120:**647–662

Zhou, Y., Morais-Cabral, J.H., Kaufman, A., MacKinnon, R. 2001b. Chemistry of ion coordination and hydration revealed by a K^+ channel-Fab complex at 2.0 Å resolution. *Nature* **414:**43–48